Lysozyme encapsulated gold nanoclusters for probing the early stage of lysozyme aggregation under acidic conditions

Nora Alkudaisi[a], Ben Allan Russell[a], David J. S. Birch[a] and Yu Chen[a,*]

[a]Physics department, University of Strathclyde, Glasgow, UK

*corresponding author: y.chen@strath.ac.uk

Abstract

Protein aggregation can lead to several incurable amyloidosis diseases. The full aggregation pathway is not fully understood, creating the need for new methods of studying this important biological phenomenon. Lysozyme is an amyloidogenic protein which is often used as a model protein for studying amyloidosis. This work explores the potential of employing Lysozyme encapsulated gold nanoclusters (Ly-AuNCs) to study the protein's aggregation. The fluorescence emission properties of Ly-AuNCs were studied in the presence of increasing concentrations of native lysozyme and as a function of pH, of relevance in macromolecular crowding and inflammation-triggered aggregation. AuNC fluorescence was observed to both redshift and increase in intensity as pH is increased or when native lysozyme is added to a solution of Ly-AuNCs at pH 3. The long (μs) fluorescence lifetime component of AuNC emission was observed to decrease under both conditions. Interestingly it was found via Time Resolved Emission Spectra (TRES) that both AuNC fluorescence components increase in intensity and redshift with increasing pH while only the long lifetime component of AuNC was observed to change when adding native lysozyme to solution; indicating that the underlying mechanisms for the changes observed are fundamentally different for each case. It is possible that the sensitivity of Ly-AuNCs to native lysozyme concentration could be utilized to study early stage aggregation.

Keywords

Gold Nanoclusters, Lysozyme, Protein Aggregation, Fluorescence

Introduction

Age related diseases such as Alzheimer's have become more prevalent in well-developed countries over time as the life expectancy of the average citizen has increased[1]. With an increasingly aging population the likelihood of citizens developing Alzheimer's is also increasing and as such the need to develop a better understanding of the underlying mechanisms, more effective therapeutics and preventative measures for an increasing number of sufferers is critical[2]. To develop effective treatments, it is first necessary to understand the cause of the disease. Several theories have been presented as to the cause of Alzheimer's including head injury[3], infection[4], exposure to toxic substances[5] and incorrect immune system responses[6]. However, the theory that has gained the most support is the Amyloid Cascade hypothesis which proposes the formation of amyloid fibrils when the protein beta amyloid is deposited in the brain[7,8]. A fundamental understanding of protein aggregation is also vital in understanding the causes and developing therapeutics for other human diseases, including Huntington's, Parkinson's, Type II diabetes and several forms of cancer[9–12]. Although diverse in nature, these diseases are attributed to a complex aggregation of proteins that are normally soluble[13]. Much effort has been put into understanding the formation of amyloid fibrils, using different techniques including fluorescence spectroscopy with extrinsic probes such as thioflavin T (ThT)[14] or tyrosine

as an intrinsic probe[15], the development of computer simulations mimicking amyloid fibril formation[16] and solid state imaging of structure formation[17] by Nuclear Magnetic Resonance. However, new methods of observing the early stages of the fibril formation are still sorely needed as these could lead to a breakthrough in understanding and downstream benefits to healthcare.

Protein encapsulated gold nanoclusters (AuNCs) are a new type of fluorescent nanoprobe which could be used to study early stage protein aggregation in addition to previous uses in metal ion, small molecule and enzyme detection[18–23]. These probes have been shown to be highly stable[24], non-photobleaching[25,26], and possess long lifetime fluorescence emission in the near red/near infrared[27]. They are also non-toxic and retain protein functionality after synthesis[21], making them ideal for studying protein aggregation with minimal probe perturbation. Lysozyme is an amyloidogenic protein which is often used as a model protein for studying amyloidosis[28]. Aggregation of lysozyme protein has been studied under various aggregation-inducing conditions such as changing pH[29,30], increase in temperature[31] and interactions with aggregate inducing molecules such as guanidine hydrochloride and urea[32]. Previously lysozyme has been successfully used as a scaffold for AuNC (Ly-AuNCs) synthesis and as such opens questions as to whether AuNC fluorescence from Ly-AuNCs can be used to monitor lysozyme aggregation and better understand the formation of amyloid fibrils. A recent study found that macromolecular crowding in living cells significantly impacted on the structure of protein and led to its aggregation[33]. Moreover, there is growing body of evidence suggesting that inflammation plays an important role in the development of Alzheimer's disease[34]. pH dependent aggregation is relevant in inflammation-triggered aggregation as well as in secondary nucleation of monomers in endosomes and other organelles of relevance to Parkinson's disease[35]. Here, we studied the fluorescence emission properties of Ly-AuNCs in the presence of increasing concentrations of native lysozyme and as a function of pH.

Materials and Methods

Lysozyme (crystallized and lyophilized powder, from chicken egg white, (HEWL)), (≥99%) and Gold(III) Chloride Hydrate and Phosphate Buffer Solution in tablet form (PBS) were purchased from Sigma Aldrich while all other chemicals used during the study were purchased from Fluka and used without further purification. The synthesis of Lysozyme-AuNCs (Ly-AuNCs) was carried out using a modified version of Xie's one-pot method by Wei *et. al.*[36]. Initially, a 5 ml solution of 10 mg ml^{-1} Lysozyme was mixed with a 5 ml solution of 4 mM $HAuCl_4$ and 5 ml of H_2O at 37 ^{O}C for 5 minutes. Next 0.5 ml of 1 M NaOH was added to the solution and incubated at 37 ^{O}C for 7 hours. The solution was then iincubated without stirring for a further 48 hours at 37 ^{O}C. Ly-AuNCs were then dialysed into PBS buffer solution using 10kDa dialysis cassettes to remove any impurities from solution. The pH was altered using Hydrochloric acid and Sodium Hydroxide.

Fluorescence emission spectra were measured using a HORIBA Fluorolog 3. Fluorescence lifetimes were measured using Time Correlated Single Photon Counting (TCSPC) with a HORIBA Deltaflex. For all measurements, a time range of 13 μs was used with 482 nm HORIBA DeltaDiode laser excitation. All curves were measured until a peak count of 10,000 was obtained. Data were analysed using the DAS6 software package supplied by HORIBA. TRES and fluorescence anisotropy measurements were obtained using the same equipment and software package. The fluorescence intensity associated with a fluorescence decay component, i, was calculated from the product of the decay time τ_i and the amplitude β_i obtained from the non-linear least-squares reconvolution analysis of the decay data.

Results & Discussion

Initially the fluorescence properties of Ly-AuNCs were studied at different pH values, the sample being excited at 470 nm (S.1 in supporting Information). The emission of AuNCs via 470 nm excitation produced an increase in fluorescence intensity at high pH compared to low pH and the peak emission wavelength was seen to red shift at high pH. The small intensity fluctuation in the pH range between 7-12 was mainly due to the experimental uncertainty. The pH range between 3.5 – 6 was avoided in all the experiments due to the formation of large aggregates which are opaque[29]. The results for exciting at 470 nm are shown in Figure 1.

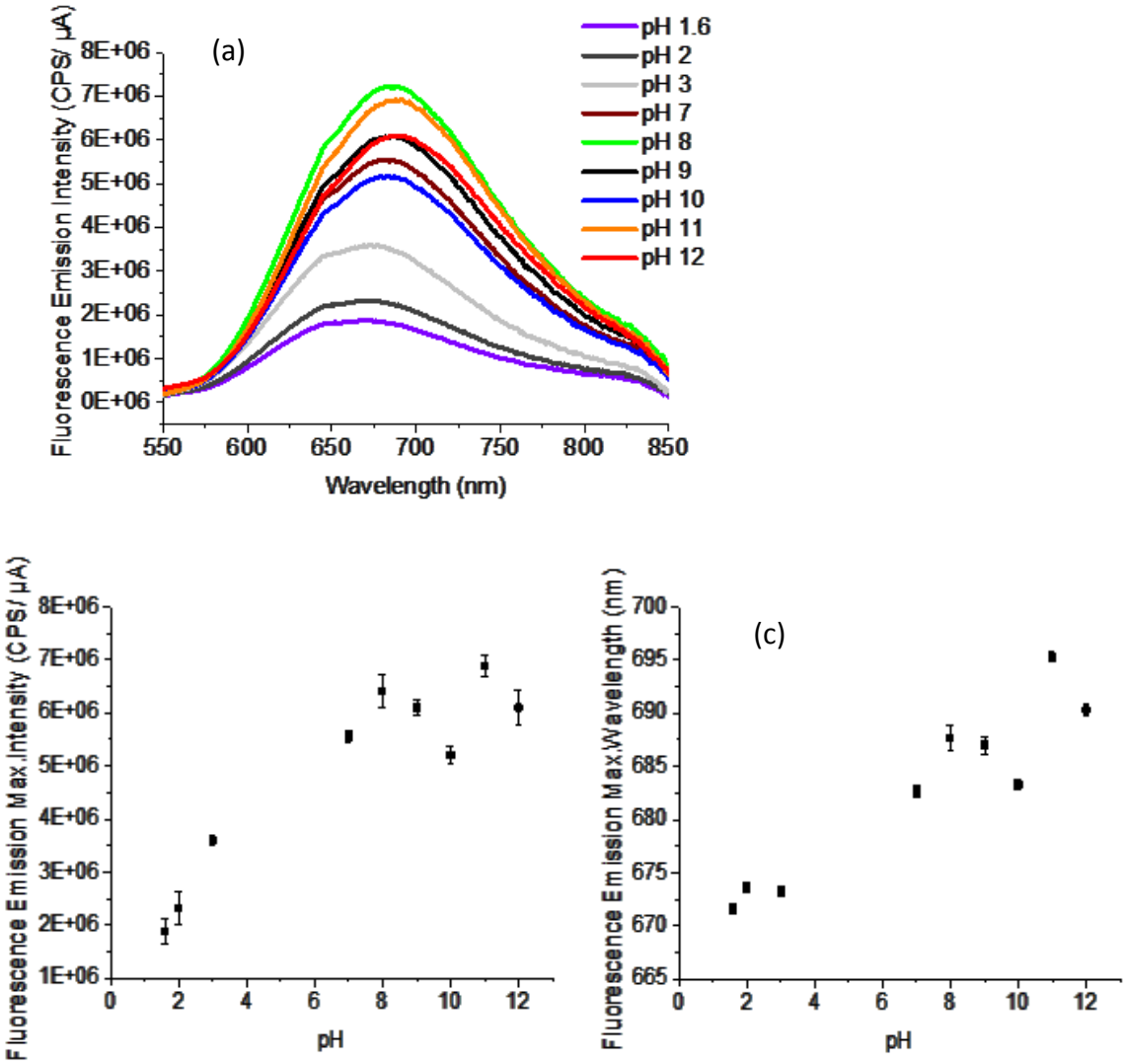

Figure 1: pH dependence of (a) fluorescence emission spectra, (b) peak fluorescence emission and (c) peak emission wavelength. The excitation wavelength is 470 nm.

Previously, Cao *et. al.* observed the fluorescence changes in Bovine Serum Albumin (BSA) encapsulated AuNCs as a function of pH. It was found that the intensity of AuNC emission in the red spectrum regime increased progressively and the peak emission wavelength also increased between pH 2 – 11 while exciting at 500 nm[37] The large red-shift in fluorescence emission due to pH has also previously been observed for BSA-AuNCs by Wen *et. al.*[38]. The red-shift was attributed to the Quantum Confined Stark Effect (QCSE). QCSE is the shifting of electrons in a quantum well to lower discrete energy levels in the presence of an external electric field, while increasing the discrete hole states of a system to higher energies[39]. Due to the polar nature of the Ly-AuNC molecules and the highly negative zeta potential of Ly-AuNCs previously reported to be greater than negative 60 mV below pH 11[29] it is possible the redshift is governed by the polar characteristics of QCSE which have been observed arising in similar fluorescence quantum dot systems[40–42]. However, the fluorescence emission intensity would be expected to decrease if QCSE was the reason for the observed fluorescence red-shift for Ly-AuNCs. Wen *et. al.* have also observed a two-band fluorescence emission from BSA-AuNCs, describing the AuNC with a "core/shell " fluorescence model derived from thiolate-protected Au_{25} in which the core and shell are each responsible for a fluorescence band which makes up the red fluorescence peak[38,43,44]. This core/shell structure originates from the metal core state and surface states of the SR – Au – SR – Au – SR staples, respectively. AuNC in BSA binds to sulphur (S) atoms (via cysteine) but with a much

reduced number than that in thiolate-protected Au_{25}.[27] Although the exact atomic structure is unknown, S-Au bonds (and possible bonds of gold to other neighbouring amino acids) form a motif that stabilizes the gold core. It is plausible that two emission bands have different structural characteristics and different sensitivity to local environmental changes.

The fluorescence lifetimes of protein encapsulated AuNCs are 2 exponential in nature[21,40,41], which compares well to the idea of a two band fluorescence emission model. To gain further understanding on the behaviour of Ly-AuNCs fluorescence due to changing pH, the fluorescence lifetimes of Ly-AuNCs were measured at different pH, excited directly at 482 nm and emission collected at 650 nm. At neutral pH, the fluorescence decay was found to be 2-exponential in nature; 2 long lifetimes associated with the fluorescence of the AuNCs of τ_1 = 2057 ± 7 ns and τ_2 = 723 ± 23 ns, similar to as previously reported from other AuNCs[27] plus one very fast component associated with scattered light from the sample itself. It was found from Figure 2 that as pH is increased, the longer lifetime, τ_1, clearly decreases from 2.4 to 2.0 μs, while τ_2 may show a small increase but remains within the uncertainty associated with the measurement. This has been previously observed in BSA-AuNCs[27] where changing pH results in protein unfolding, thus changing of local environment of the AuNCs. Lysozyme is more rigid but AuNC is more exposed to the solvent in comparison to that in HSA, and is therefore more sensitive to pH variation.

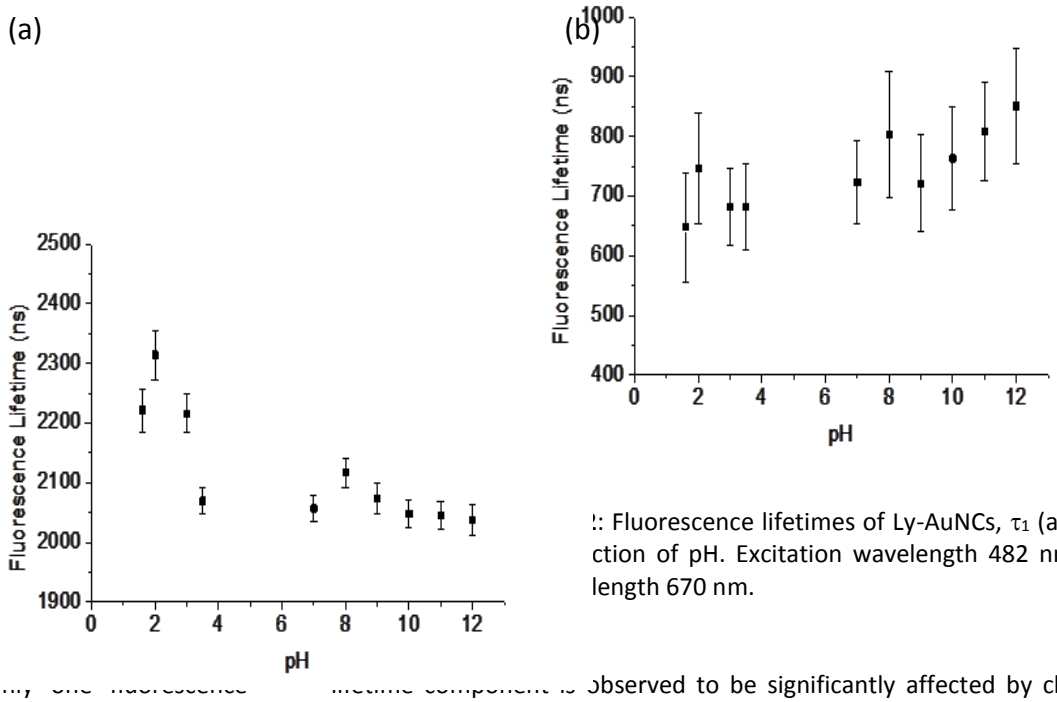

!: Fluorescence lifetimes of Ly-AuNCs, τ_1 (a) and τ_2 (b), ction of pH. Excitation wavelength 482 nm, emission length 670 nm.

Only one fluorescence lifetime component is observed to be significantly affected by changing pH. The increase in the fluorescence intensity correlated to the decrease of fluorescence lifetime suggests that this is not due to a reduced collisional quenching effect but possibly a mechanism of enhanced radiative process arising in a basic environment.

To further understand the correlation between the two fluorescence components and the overall increase in intensity and redshift previously observed, TRES measurements were taken of Ly-AuNCs emission at pH 3 and pH 7, as shown in Figure 3. Interestingly the TRES show both components increase in intensity and redshift, despite the decrease in fluorescence lifetime for the longer-lived fluorescence component. Previously, changes in the relative intensity of the two bands at different pH was observed[27]. TRES of Bovine Serum Albumin encapsulated AuNCs (BSA-AuNC) has shown two emission bands of 650 nm and 680 nm corresponding to τ = 2.40 μs and τ = 1.17 μs at pH 12, and emission bands at 620 nm and 640 nm with corresponding to lifetimes of τ = 4.46 μs and τ = 1.94 μs[27] at pH 3.

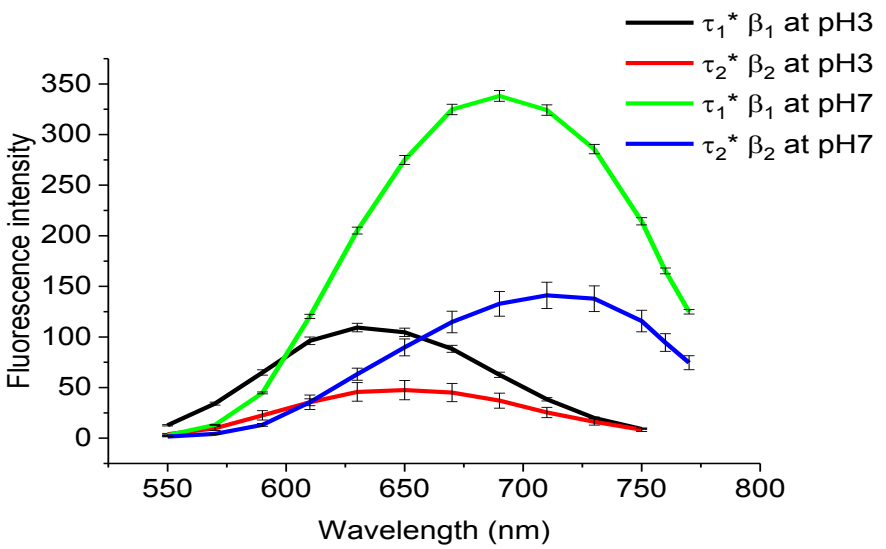

Figure 3: TRES of Ly-AuNCs in solution at pH 3 and pH 7. The excitation wavelength is 482 nm.

To test the sensitivity of Ly-AuNC fluorescence to native protein interactions, lysozyme was added to a solution of Ly-AuNCs and the fluorescence characteristics were observed. Two conditions of pH 3 and 12.5, were chosen due to them being either side of the isoelectric point of Ly-AuNCs and the fluorescence emission characteristics were monitored upon introducing increasing concentrations of native lysozyme to the solution. The Ly-AuNCs were excited at 470 nm and small increments of native lysozyme were added; the results are shown in Figure 4.

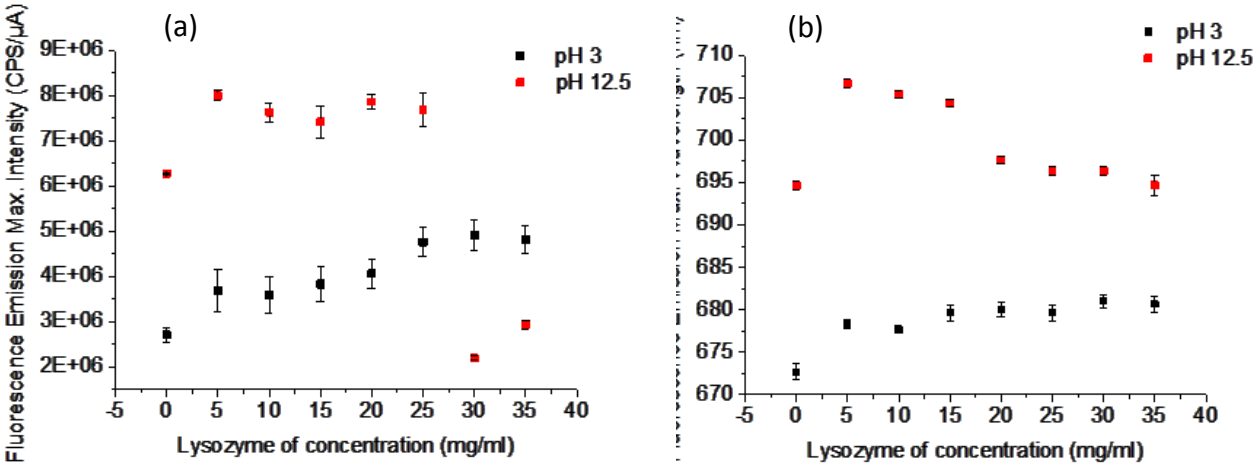

Figure 4: Fluorescence emission spectrum maximum intensity of Ly-AuNCs (a) and fluorescence emission maximum wavelength (b) at different pH (pH 3 indicated in black, pH 12.5 indicated in red) as a function of native lysozyme addition in solution. The excitation wavelength is 470 nm. (Note that integrating the fluorescence intensity over all wavelengths showed similar trends).

A small and gradual increase in fluorescence emission was observed at pH 3. A red-shift in fluorescence emission wavelength was observed upon first adding 5 mg/ml lysozyme to solution from 673 nm to 678 nm. Further increases in lysozyme concentration in solution yielded no clear further changes in fluorescence wavelength. No clear trend was evident for changes observed with the sample at pH 12.5. Clearly fluorescence emission intensity characteristics were not as sensitive or as unambiguous a method of probing protein/protein interactions where precipitation due to the formation of large aggregates results in changes in particle concentration. Therefore, fluorescence emission lifetimes were studied upon adding native lysozyme

to Ly-AuNCs to determine any sensitivity of Ly-AuNCs to protein/protein interactions at both pH 3 and pH 12.5. It was found that at pH 3 the longer fluorescence lifetime, τ_1, linearly decreased from 2.13 μs to 1.85 μs between 0-30 mg/ml added. No changes in τ_2 at pH 3 as lysozyme is added to the Ly-AuNCs solution were detected within the measurement error. At pH 12.5 both fluorescence lifetimes were observed to be unaffected by the addition of native lysozyme to the Ly-AuNCs solution. The results are shown in Figure 5.

Figure 5: Fluorescence lifetimes of Ly-AuNCs as a function of added native lysozyme to solution and different pH. Ly-AuNCs τ_1 at pH 3 (a), Ly-AuNCs τ_2 at pH 3 (b), Ly-AuNCs τ_1 at pH 12.5 (c), Ly-AuNCs τ_2 at pH 12.5 (d). The excitation wavelength is 482 nm.

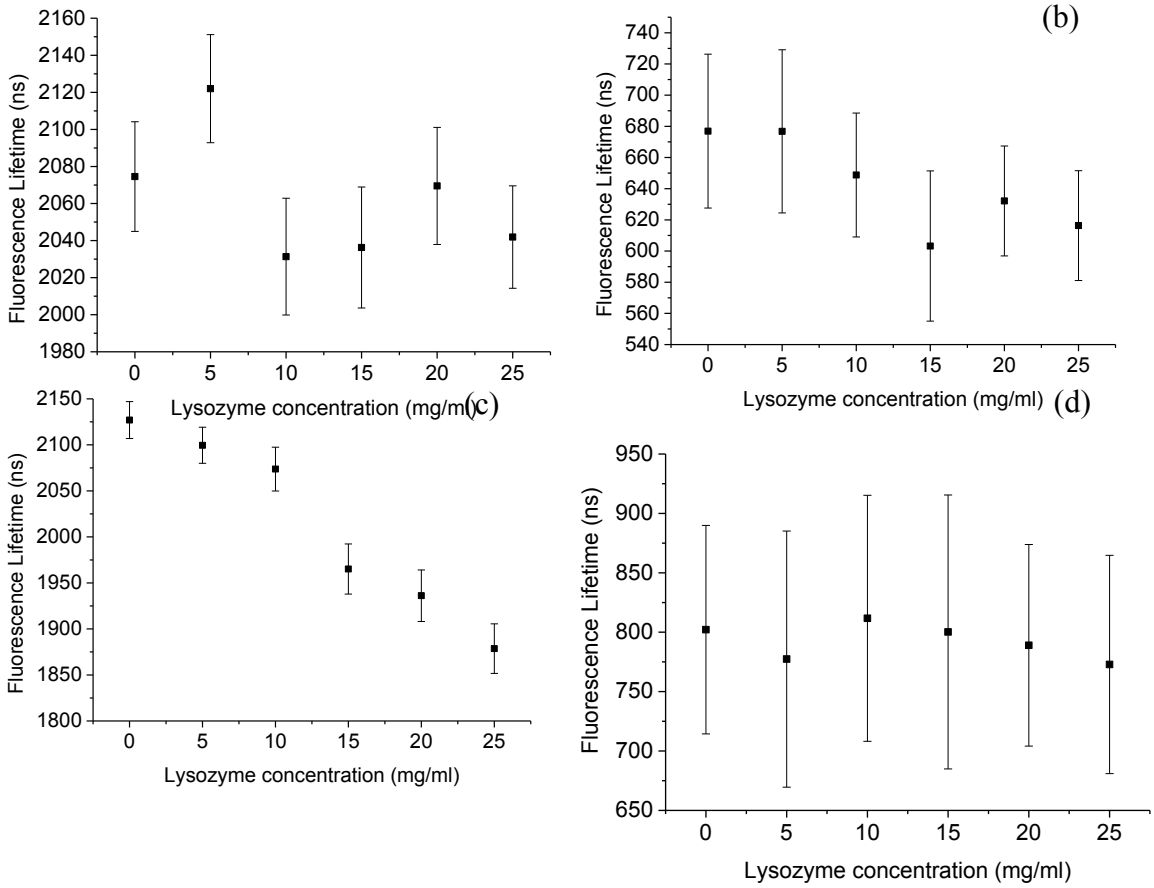

Again, it is the longer lifetime component which is sensitive to environmental changes at pH 3. The lack of sensitivity at pH 12.5 suggests that the interaction between Ly-AuNCs and native lysozyme does not affect the micro-environment in which the AuNC is located within the lysozyme-AuNC complex. Time-resolved fluorescence anisotropy of the Ly-AuNCs at pH 3 and pH 12.5 in the presence and absence of native lysozyme was carried out to observe whether aggregation took place. Previous studies reported a loss of alpha helicity after the synthesis of encapsulated AuNC in lysozyme [46] and formation of dimmer [24]. The hydrodynamic radii of the Ly-AuNCs was found to be 3.73 ± 0.8 nm at pH 3 and 3.84 ± 0.52 nm at pH 12.5; comparing well with previously reported values[29]. An increase in the hydrodynamic radii to 6.49 ± 1.28 nm was observed upon adding 25 mg/ml of native lysozyme to Ly-AuNCs at pH 3. Interestingly, an increase in hydrodynamic radius to 5.86 ± 1.37nm at pH 12.5 was also observed. The difference in hydrodynamic radii indicates that the Ly-AuNCs and native lysozyme begin to form small initial aggregates of 2 – 4 protein molecules in size at pH 3 and pH 12.5 in different conformations. This perhaps is not too surprising since Ly-AuNCs and lysozyme have a similar positive zeta potential at pH 3 whereas in highly basic conditions lysozyme has a weak negative zeta potential and Ly-AuNCs have a very strong negative zeta potential[29]. It has been previously shown by Burnett *et. al.* that environmental conditions affect the aggregate morphologies of lysozyme and as such supports the theory that the differences observed in fluorescence lifetimes for Ly-AuNCs under different pH

conditions may arise from different aggregation forms[42]. It is possible that the reason for a decrease in τ_1 at pH 3 is due to the binding of native lysozyme to Ly-AuNCs near the AuNC nucleation sites and shielding of AuNC from the acidic environment, thus resulting in enhancement of the radiative rate. To better understand the fluorescence mechanics when adding lysozyme to Ly-AuNCs at pH 3, the TRES of AuNCs was measured in the presence and absence of native lysozyme in solution, as shown in Figure 6.

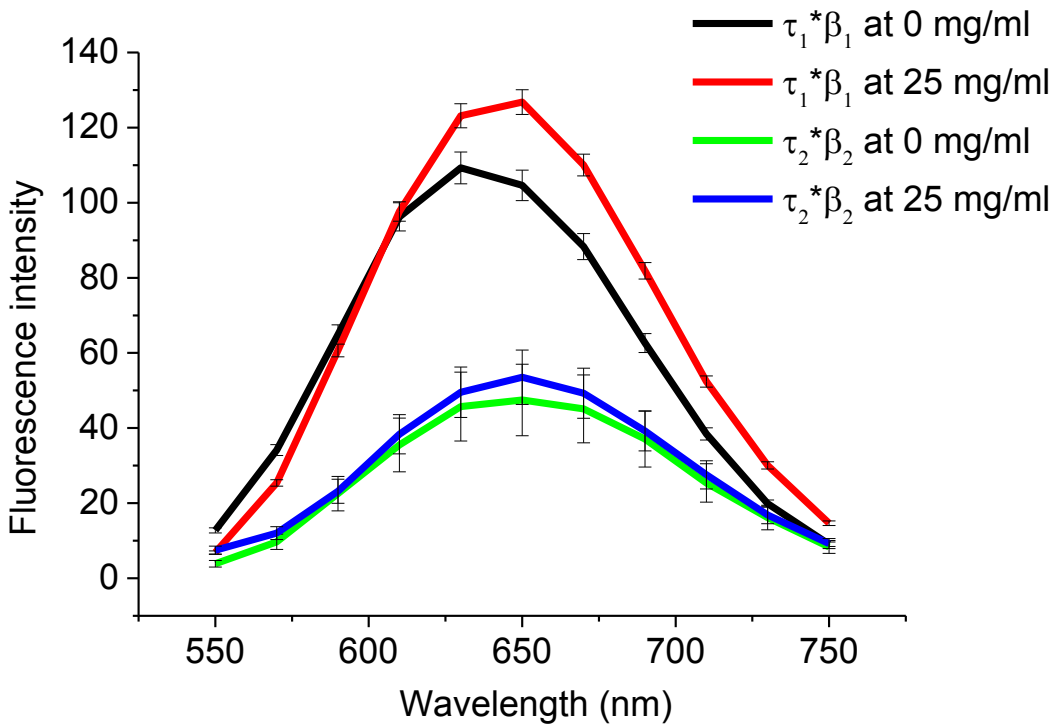

Figure 6: Time resolved emission spectra of Ly-AuNCs in the presence and absence of native lysozyme in solution at pH 3. The excitation wavelength is 482 nm.

From Figure 6 we can see that the longer lifetime τ_1 emission increases and redshifts, while the emission from τ_2 remains unchanged; confirming that the smaller fluorescence increase and redshift seen previously in Figure 4 can be directly attributed to the changes in the fluorescence emission of τ_1. Comparing this to the previous TRES measurements of Figure 3, we can see that while the changes in the fluorescence emission spectra and fluorescence emission lifetimes are similar for increasing pH and adding native lysozyme to solution, the underlying mechanism for these observations is different. In the case of increasing pH we observe a large intensity increase and redshift for both fluorescence components whereas upon adding native lysozyme to solution only τ_1 undergoes a slight increase in intensity and redshift. Previously we have observed that the diameter of Ly-AuNCs remains quite consistent at 8.0 nm across a pH range of 2-11 (with the exception of aggregates forming around the isoelectric point of Ly-AuNCs at pH 4[29]. Therefore, we can rule out the formation of aggregates as the reason for the observed fluorescence changes. It is more likely that the observed changes to both τ_1 and τ_2 are caused electrostatically, since the Ly-AuNC complex has been observed to become more negatively charged at higher pH. However, in the case of adding native lysozyme to the Ly-AuNC solution, it is more plausible that the observed changes in fluorescence characteristics are due to the formation of small initial proto-aggregates of 2 – 4 proteins in size. Previously Siddiqui *et. al.* have shown the increase and redshift of intrinsic hemagloblin fluorescence upon macromolecular crowding and aggregation caused by bovine serum albumin (BSA) interaction[33]. Initial aggregate formation alone however did not result in changes to the fluorescence characteristics of AuNCs at pH 12.5 when adding native lysozyme, only at pH 3, therefore the aggregation morphology must play an important role since the morphology at pH 3 and pH 12.5 can be expected to be different due to changes in protein surface charge and interaction of lysozyme[33]. Therefore, it seems likely that the changes to τ_1 only arise from a physical interaction of the AuNCs with the surrounding microenvironment due to initial aggregate induced conformational changes.

Conclusions

Here we have presented the environmental induced effects of Ly-AuNCs fluorescence characteristics including fluorescence emission intensity, peak emission wavelength, fluorescence lifetime and time resolved emission. It was found that the fluorescence emission intensity and peak fluorescence wavelength of Ly-AuNCs increases and red-shifts upon changing pH from acidic to basic conditions when exciting the AuNC directly at 470 nm. The longer fluorescence lifetime component τ_1 was also seen to decrease in highly basic conditions. We have also reported the interaction between Ly-AuNCs and varying concentrations at different pH. Clear changes to the fluorescence characteristics of Ly-AuNCs were observed at pH 3, with the fluorescence emission intensity increasing linearly with native lysozyme concentration, a small redshift in peak wavelength and a decrease in the τ_1 fluorescence lifetime. Conversely no clear trend was observed at pH 12.5 for Ly-AuNCs fluorescence. This is thought to be due to differences in the small aggregate morphology at pH 3 and pH 12.5 as Ly-AuNC-native lysozyme proto-aggregates begin to form. Further studies are needed to determine the exact nature of Ly-AuNCs-native lysozyme proto-aggregate formations; however, these initial results show the sensitivity of Ly-AuNCs to environmental changes and early aggregation, which may be utilized in the future as a means of studying and modelling lysozyme aggregation.

Acknowledgements

Nora Alkudaisi acknowledges a PhD Studentship from the Saudi Arabian Cultural Bureau.

References

[1] C. Qiu, M. Kivipelto, E. von Strauss, Epidemiology of Alzheimer's disease: occurrence, determinants, and strategies toward intervention, Dialogues Clin. Neurosci. 11 (2009) 111–128.

[2] A.D. Korczyn, Why have we failed to cure Alzheimer's disease?, J. Alzheimers. Dis. 29 (2012) 275–282. doi:10.3233/JAD-2011-110359.

[3] Y. Li, Y. Li, X. Li, S. Zhang, J. Zhao, X. Zhu, G. Tian, Head Injury as a Risk Factor for Dementia and Alzheimer's Disease: A Systematic Review and Meta-Analysis of 32 Observational Studies, PLoS One. 12 (2017) e0169650. doi:10.1371/journal.pone.0169650.

[4] F. Bibi, M. Yasir, S.S. Sohrab, E.I. Azhar, M.H. Al-Qahtani, A.M. Abuzenadah, M.A. Kamal, M.I. Naseer, Link between chronic bacterial inflammation and Alzheimer disease., CNS Neurol. Disord. Drug Targets. 13 (2014) 1140–1147.

[5] L. Tomljenovic, Aluminum and Alzheimer's disease: after a century of controversy, is there a plausible link?, J. Alzheimers. Dis. 23 (2011) 567–598. doi:10.3233/JAD-2010-101494.

[6] T. Fulop, A.Y. Le Page, E.H. Frost, G. Dupuis, Role of the innate immune response in the progression of Alzheimer's disease, J. Immunol. 198 (2017) 55.27 LP-55.27.

[7] J.A. Hardy, G.A. Higgins, Alzheimer's disease: the amyloid cascade hypothesis, Science (80-.). 256 (1992) 184 LP – 185.

[8] E. Karran, M. Mercken, B. De Strooper, The amyloid cascade hypothesis for Alzheimer's disease: an appraisal for the development of therapeutics, Nat. Rev. Drug Discov. 10 (2011) 698.

[9] T. Scheibel, J. Buchner, Protein Aggregation as a Cause for Disease, in: K. Starke, M. Gaestel (Eds.), Mol. Chaperones Heal. Dis., Springer Berlin Heidelberg, Berlin, Heidelberg, 2006: pp. 199–219. doi:10.1007/3-540-29717-0_9.

[10] A. Aguzzi, T. O'Connor, Protein aggregation diseases: pathogenicity and therapeutic perspectives, Nat. Rev. Drug Discov. 9 (2010) 237.

[11] C.A. Ross, M.A. Poirier, Protein aggregation and neurodegenerative disease., Nat. Med. 10 Suppl (2004) S10-7. doi:10.1038/nm1066.

[12] B.A. Russell, B. Jachimska, I. Kralka, P.A. Mulheran, Y. Chen, Human serum albumin encapsulated gold nanoclusters: effects of cluster synthesis on natural protein characteristics, J. Mater. Chem. B. 4 (2016)

6876–6882. doi:10.1039/C6TB01827K.
[13] C.M. Dobson, The structural basis of protein folding and its links with human disease., Philos. Trans. R. Soc. Lond. B. Biol. Sci. 356 (2001) 133–45. doi:10.1098/rstb.2000.0758.
[14] A.M. Streets, Y. Sourigues, R.R. Kopito, R. Melki, S.R. Quake, Simultaneous Measurement of Amyloid Fibril Formation by Dynamic Light Scattering and Fluorescence Reveals Complex Aggregation Kinetics, PLoS One. 8 (2013) 1–10. doi:10.1371/journal.pone.0054541.
[15] O.J. Rolinski, T. Wellbrock, D.J.S. Birch, V. Vyshemirsky, Tyrosine Photophysics during the Early Stages of ?-Amyloid Aggregation Leading to Alzheimer's, J. Phys. Chem. Lett. 6 (2015) 3116–3120. doi:10.1021/acs.jpclett.5b01285.
[16] J. Nasica-Labouze, P.H. Nguyen, F. Sterpone, O. Berthoumieu, N.-V. Buchete, S. Coté, A. De Simone, A.J. Doig, P. Faller, A. Garcia, A. Laio, M.S. Li, S. Melchionna, N. Mousseau, Y. Mu, A. Paravastu, S. Pasquali, D.J. Rosenman, B. Strodel, B. Tarus, J.H. Viles, T. Zhang, C. Wang, P. Derreumaux, Amyloid β Protein and Alzheimer's Disease: When Computer Simulations Complement Experimental Studies, Chem. Rev. 115 (2015) 3518–3563. doi:10.1021/cr500638n.
[17] Y. Suzuki, J.R. Brender, M.T. Soper, J. Krishnamoorthy, Y. Zhou, B.T. Ruotolo, N.A. Kotov, A. Ramamoorthy, E.N.G. Marsh, Resolution of Oligomeric Species during the Aggregation of Aβ(1-40) Using (19)F NMR, Biochemistry. 52 (2013) 1903–1912. doi:10.1021/bi400027y.
[18] K. Shanmugaraj, M. Ilanchelian, A "turn-off" fluorescent sensor for the selective and sensitive detection of copper(ii) ions using lysozyme stabilized gold nanoclusters, RSC Adv. 6 (2016) 54518–54524. doi:10.1039/C6RA08325K.
[19] Y. Lin, W. Tseng, Ultrasensitive Sensing of Hg 2 + and CH 3 Hg + Based on the Fluorescence Quenching of Lysozyme Type VI-Stabilized Gold Nanoclusters, Anal. Chem. 82 (2010) 9194–9200.
[20] D. Lu, L. Liu, F. Li, S. Shuang, Y. Li, M.M.F. Choi, C. Dong, Lysozyme-stabilized gold nanoclusters as a novel fluorescence probe for cyanide recognition, Spectrochim. Acta Part A Mol. Biomol. Spectrosc. 121 (2014) 77–80. doi:https://doi.org/10.1016/j.saa.2013.10.009.
[21] J. Liu, L. Lu, S. Xu, L. Wang, One-pot synthesis of gold nanoclusters with bright red fluorescence and good biorecognition Abilities for visualization fluorescence enhancement detection of E. coli, Talanta. 134 (2015) 54–59. doi:10.1016/j.talanta.2014.10.058.
[22] K. Selvaprakash, Y.-C. Chen, Using protein-encapsulated gold nanoclusters as photoluminescent sensing probes for biomolecules, Biosens. Bioelectron. 61 (2014) 88–94. doi:https://doi.org/10.1016/j.bios.2014.04.055.
[23] W. Li, Z. Gao, R. Su, W. Qi, L. Wang, Z. He, Scissor-based fluorescent detection of pepsin using lysozyme-stabilized Au nanoclusters(SI)., Anal. Methods. 6 (2014) 3–4. doi:10.1039/C4AY00983E.
[24] Y. Xu, J. Sherwood, Y. Qin, D. Crowley, M. Bonizzoni, Y. Bao, The role of protein characteristics in the formation and fluorescence of Au nanoclusters, Nanoscale. 6 (2014) 1515–1524. doi:10.1039/c3nr06040c.
[25] L.Y. Chen, C.W. Wang, Z. Yuan, H.T. Chang, Fluorescent gold nanoclusters: Recent advances in sensing and imaging, Anal. Chem. 87 (2015) 216–229. doi:10.1021/ac503636j.
[26] B.A. Russell, P.A. Mulheran, D.J.S. Birch, Y. Chen, Probing the Sudlow binding site with warfarin : how does gold nanocluster growth alter human serum albumin ?, Phys. Chem. Chem. Phys. 18 (2016) 22874–22878. doi:10.1039/C6CP03428D.
[27] B.A. Russell, K. Kubiak-Ossowska, P.A. Mulheran, D.J.S. Birch, Y. Chen, Locating the Nucleation Sites for Protein Encapsulated Gold Nanoclusters: A Molecular Dynamics and Fluorescence Study, Phys. Chem. Chem. Phys. 17 (2015) 21935–21941. doi:10.1039/C5CP02380G.
[28] R. Swaminathan, V.K. Ravi, S. Kumar, M.V.S. Kumar, N. Chandra, Lysozyme: a model protein for amyloid research., Adv. Protein Chem. Struct. Biol. 84 (2011) 63–111. doi:10.1016/B978-0-12-386483-3.00003-3.
[29] B.A. Russell, B. Jachimska, P. Komorek, P.A. Mulheran, Y. Chen, Lysozyme encapsulated gold nanoclusters: Effects of cluster synthesis on natural protein characteristics, Phys. Chem. Chem. Phys. 19 (2017). doi:10.1039/c7cp00540g.
[30] W.S. Price, F. Tsuchiya, Y. Arata, Lysozyme Aggregation and Solution Properties Studied Using PGSE NMR Diffusion Measurements, J. Am. Chem. Soc. 121 (1999) 11503–11512. doi:10.1021/ja992265n.
[31] L.N. Arnaudov, R. de Vries, Thermally Induced Fibrillar Aggregation of Hen Egg White Lysozyme, Biophys. J. 88 (2005) 515–526. doi:10.1529/biophysj.104.048819.
[32] S. Emadi, M. Behzadi, A comparative study on the aggregating effects of guanidine thiocyanate, guanidine hydrochloride and urea on lysozyme aggregation., Biochem. Biophys. Res. Commun. 450 (2014) 1339–1344. doi:10.1016/j.bbrc.2014.06.133.

[33] G.A. Siddiqui, A. Naeem, Aggregation of globular protein as a consequences of macromolecular crowding: A time and concentration dependent study, Int. J. Biol. Macromol. 108 (2018) 360–366. doi:10.1016/j.ijbiomac.2017.12.001.
[34] A.P. Mann, P. Scodeller, S. Hussain, G.B. Braun, T. Mölder, K. Toome, R. Ambasudhan, T. Teesalu, S.A. Lipton, E. Ruoslahti, Identification of a peptide recognizing cerebrovascular changes in mouse models of Alzheimer's disease, Nat. Commun. 8 (2017). doi:10.1038/s41467-017-01096-0.
[35] R. Gaspar, G. Meisl, A.K. Buell, L. Young, C.F. Kaminski, T.P.J. Knowles, E. Sparr, S. Linse, Secondary nucleation of monomers on fibril surface dominates α-synuclein aggregation and provides autocatalytic amyloid amplification, Q. Rev. Biophys. 50 (2017). doi:10.1017/S0033583516000172.
[36] H. Wei, Z. Wang, J. Zhang, S. House, Y.-G. Gao, L. Yang, H. Robinson, L.H. Tan, H. Xing, C. Hou, I.M. Robertson, J.-M. Zuo, Y. Lu, Time-dependent, protein-directed growth of gold nanoparticles within a single crystal of lysozyme., Nat. Nanotechnol. 6 (2011) 93–97. doi:10.1038/nnano.2010.280.
[37] X.-L.L. Cao, H.-W.W. Li, Y. Yue, Y. Wu, pH-Induced conformational changes of BSA in fluorescent AuNCs@BSA and its effects on NCs emission, Vib. Spectrosc. 65 (2013) 186–192. doi:10.1016/j.vibspec.2013.01.004.
[38] X. Wen, P. Yu, Y.R. Toh, J. Tang, Structure-correlated dual fluorescent bands in BSA-protected Au25 nanoclusters, J. Phys. Chem. C. 116 (2012) 11830–11836. doi:10.1021/jp303530h.
[39] D.A.B. Miller, D.S. Chemla, T.C. Damen, A.C. Gossard, W. Wiegmann, T.H. Wood, C.A. Burrus, Band-Edge Electroabsorption in Quantum Well Structures: The Quantum-Confined Stark Effect, Phys. Rev. Lett. 53 (1984) 2173–2176. doi:10.1103/PhysRevLett.53.2173.
[40] G.W. Wen, J.Y. Lin, H.X. Jiang, Z. Chen, Quantum-confined Stark effects in semiconductor quantum dots, Phys. Rev. B. 52 (1995) 5913–5922. doi:10.1103/PhysRevB.52.5913.
[41] J.W. Robinson, J.H. Rice, K.H. Lee, J.H. Na, R.A. Taylor, D.G. Hasko, R.A. Oliver, M.J. Kappers, C.J. Humphreys, G.A.D. Briggs, Quantum-confined Stark effect in a single InGaN quantum dot under a lateral electric field, Appl. Phys. Lett. 86 (2005) 213103. doi:10.1063/1.1935044.
[42] S.A. Empedocles, M.G. Bawendi, Quantum-Confined Stark Effect in Single CdSe Nanocrystallite Quantum Dots, Science (80-.). 278 (1997) 2114 LP – 2117.
[43] J. Akola, M. Walter, R.L. Whetten, H. Häkkinen, H. Grönbeck, On the Structure of Thiolate-Protected Au25, J. Am. Chem. Soc. 130 (2008) 3756–3757. doi:10.1021/ja800594p.
[44] Z. Luo, X. Yuan, Y. Yu, Q. Zhang, D.T. Leong, J.Y. Lee, J. Xie, From Aggregation-Induced Emission of Au(I)–Thiolate Complexes to Ultrabright Au(0)@Au(I)–Thiolate Core–Shell Nanoclusters, J. Am. Chem. Soc. 134 (2012) 16662–16670. doi:10.1021/ja306199p.
[45] S. Raut, R. Chib, R. Rich, D. Shumilov, Z. Gryczynski, I. Gryczynski, Polarization properties of fluorescent BSA protected Au25 nanoclusters., Nanoscale. 5 (2013) 3441–3446. doi:10.1039/c3nr34152f.
[46] N. Alkudaisi, B.A. Russell, B. Jachimska, D.J.S. Birch, Y. Chen, Detecting lysozyme unfolding: Via the fluorescence of lysozyme encapsulated gold nanoclusters, J. Mater. Chem. B. 7 (2019) 1167–1175. doi:10.1039/c9tb00009g.
[47] L.C. Burnett, B.J. Burnett, B. Li, S.T. Durrance, S. Xu, A Lysozyme Concentration, pH, and Time-Dependent Isothermal Transformation Diagram Reveals Fibrous Amyloid and Non-Fibrous, Amorphous Aggregate Species, Open J. Biophys. 04 (2014) 39–50. doi:10.4236/ojbiphy.2014.42006.